
Entropic Lattice Boltzmann Method for high Reynolds number fluid flows

Hui Xu, Hui-Bao Luan, Gui-HuaTang
and Wen-Quan Tao*

School of Energy and Power Engineering,
Xi'an Jiao tong University,
Xi'an, Shaanxi, 710049, PR China
Fax: 86-29-8266 9106
E-mail: x_hbj@mail.xjtu.edu.cn
E-mail: hbluan@stu.xjtu.edu.cn
E-mail: ghtang@mail.xjtu.edu.cn
E-mail: wqtao@mail.xjtu.edu.cn
*Corresponding author

Abstract: The Lattice Boltzmann Method (LBM) has emerged as a computationally efficient and increasingly popular numerical method for simulating complex fluid flow. However, the standard LBM has always suffered from severe numerical instability. In this paper, we mainly focus on Entropic Lattice Boltzmann Methods (ELBM) for high Reynolds number fluid flow. ELBM, which is derived from H-theorem, enhances the numerical stability of LBM. The compliance of ELBM with H-theorem makes ELBM much more stable than the standard LBM, but the computational cost increases because of solving a non-linear equation. We propose a new optimisation strategy to improve the efficiency of ELBM, and also implement some numerical tests to validate the computational stabilities and correctness.

Keywords: LBM; lattice Boltzmann method; ELBM; entropic lattice Boltzmann method; optimisation strategies; H-theory; Lyapunov function; Lyapunov stability; entropic function.

Reference to this paper should be made as follows: Xu, H., Luan, H-B., Tang, G-H. and Tao, W-Q. (2009) 'Entropic Lattice Boltzmann Method for high Reynolds number fluid flows', *Progress in Computational Fluid Dynamics*, Vol. 9, Nos. 3/4/5, pp.183–193.

Biographical notes: Hui Xu is a PhD student in School of Energy and Power Engineering in Xi'an Jiaotong University since 2006. He got his Bachelor Degree and Master Degree from School of Science in Xi'an Jiaotong University in 2003 and 2006, respectively. Now, he focuses on multiscale problems and methods and LBMs in fluid dynamics.

Hui-Bao Luan is a PhD student in School of Energy and Power Engineering in Xi'an Jiaotong University since the spring of 2007. He got his Bachelor Degree from School of Energy and Power Engineering in Xi'an Jiaotong University in 2005. Now, he works on LBMs and porous media fluid flows.

Gui-HuaTang is an Associate Professor in School of Energy and Power Engineering in Xi'an Jiaotong University. He got his Master Degree and PhD from School of Energy and Power Engineering in Xi'an Jiaotong University in 1999 and 2004, respectively. Now, he works on microscopic fluid flows and heat transfer, multi-component multiphase fluid flows, LBMs, biological fluid flows and non-linear dynamical behaviours in porous media.

Wen-Quan Tao is a Professor of Power and Energy Engineering School at Xi'an Jiaotong University of China. His research interests include enhanced heat transfer, numerical heat transfer and micro scale heat transfer, and solar energy: science and engineering. Currently, he is the member of Chinese Academy of Science, Associate Editor of *International Journal of Heat and Mass Transfer* and *International Communications in Heat and Mass Transfer* and Vice Chairman of the Chinese Engineering Thermophysics Association.

1 Introduction

In the past decades, the Lattice Boltzmann Method (LBM) has provided a novel method to approximate the fluid flow

problems (Succi, 2001). This method is based on Boltzmann kinetic equation which is used to describe a number of interacting populations of micro-particles. This is a mesoscopic study of the macroscopic problem, into which

the basic conservation laws of the hydrodynamic variables such as mass and momentum are incorporated. The standard LBM reads (Succi, 2001; Qian et al., 1992)

$$f_i(x + e_i \delta t, t + \delta t) - f_i(x, t) = \gamma(f_i^{eq}(x, t) - f_i(x, t))$$

$$i = 0, \dots, n, \quad (1)$$

where f_i represents a single-particle distribution function along the lattice directions defined by the discrete speed set $\{e_i\}$. The left-hand side of Equation (1) f_i represents the particle-free streaming, whereas the right-hand side of Equation (1) represents particles collision via single-time relaxation towards the local equilibrium distribution function f_i^{eq} on the relaxation frequency γ . The relaxation parameter γ is a function of the single-time scale τ . The equilibrium distribution of the standard LBM is the non-entropy polynomial quasi-equilibrium (Succi, 2001). The standard LBM has been proven to be an accurate and efficient tool for simulating various non-trivial fluid dynamics problems, such as incompressible fluid flows (Succi, 2001; Li et al., 2004), turbulent flows for not very high Reynolds numbers (Chen et al., 2003), multiphase flows (Rothman and Zaleski, 1994; Chen and Doolen, 1998) and so on (Takada et al., 2001; He and Li, 2000), and has achieved successes in many practical applications. However, the standard LBM suffers from numerical instability problems (Succi, 2001; Ansumali and Karlin, 2000; Boghosian et al., 2001). Hence, flows of large Reynolds numbers in the standard LBM simulation can be simulated only by enlarging spatial grid. It is proved that to improve the stability numerical algorithm should be based on the analogue of Boltzmann H-theorem (Ansumali and Karlin, 2000; Boghosian et al., 2001). In fact, for the standard LBM, there is non-existence of the H-theorem (Yong and Luo, 2003, 2005). Recently, an isothermal LBM has been established by constructing the collision integral on the basis of the entropy function, and by stabilising the updates on the basis of the discrete H-theorem in the discrete velocity spaces (Ansumali and Karlin, 2001; Keating et al., 2007). This stabilisation method alleviates the instability limitation by restoring the second law of thermodynamics. This class of LBM is unconditionally stable and is called Entropic Lattice Boltzmann Method (ELBM).

Compared with the standard LBM, ELBM can simulate fluid flows of higher Reynolds number. Especially, when the single-particle distributions of populations are far from the equilibrium, ELBM can work very well. The standard LBM exhibits a serious numerical instability for these problems, while ELBM can improve the numerical stability and holds good numerical accuracy. However, in the scheme of ELBM, there exists a non-linear equation, which must be solved to gain the modified relaxation frequency. Thus, ELBM needs more computational CPU time compared with the standard LBM. There have been some optimisation strategies to reduce the computational cost of ELBM (Tosi et al., 2006a; Brownlee et al., 2006).

For whatever optimisation strategies being adopted, we still aim at enlarging the Reynolds number range of fluid flow problems to be simulated. The investigations of this paper concentrate on the high Reynolds number fluid flow simulation by ELBM with high efficiency. We will propose some optimisation strategy to improve the efficiencies of ELBM for flows with different Reynolds numbers. Some two-dimensional (2D) isothermal hydrodynamics will first be simulated with the proposed method and compared with benchmark solutions. Then a three-dimensional (3D) turbulent fluid flow problem will be predicted by the revised ELBM and comparisons will be given with the literature.

2 Brief review of ELBM

In this section, we will introduce the ELBM and the corresponding Boltzmann entropy function. It is well known that the single-time relaxation scheme of Equation (1) is a significant improvement in the Boltzmann kinetic equation from practical application views. The form of the single-time relaxation collision operator is the diagonal form, that is to say, the LBM scheme can be rewritten by a matrix form and the corresponding relaxation term is represented by a diagonal matrix. This fundamental LBM scheme is supported by the first principle of the thermodynamics. Generally, the positive-definiteness of f_i cannot be sustained for most flow problems at each grid node for all time. In such cases, the second principle of thermodynamics is violated. The numerical instabilities are induced by the loss of compliance with the second principle of thermodynamics (Takada et al., 2001). ELBM is a strategy to enhance the linear stability of the standard LBM scheme via the H-theorem (Tosi et al., 2006b) or entropy function. The corresponding equilibrium distribution of ELBM is suitable to recover the Navier-Stokes equations (Keating et al., 2007).

To introduce ELBM, we first give the definition of the continuous entropy function as follows (Chapman and Cowling, 1970):

$$S(f(x, v, t)) = -H(t) = -\int f(x, v, t) \ln(f(x, v, t)) dv. \quad (2)$$

The right hand of Equation (2) is the minus Boltzmann H function (Chapman and Cowling, 1970). We know that according to the Boltzmann H-theorem, the H function has the following property (Chapman and Cowling, 1970)

$$\frac{dH(t)}{dt} \leq 0.$$

In addition, for the system to reach at the equilibrium state, the essential condition is as follows:

$$\frac{dH(t)}{dt} = 0.$$

At this moment, the corresponding distribution function f_i runs to the equilibrium state and becomes the equilibrium

distribution function. According to the definition of $S(f(x, v, t))$ and the properties of Boltzmann H function, we can introduce a Lyapunov's function into the lattice Boltzmann system. On the basis of the Lyapunov's theory (Temam, 2000), we can enhance the stability of the dynamic system if we can sustain the property of the Lyapunov's function. The construction of ELBM is based on this theory. Here, we give a detailed interpretation about this. According to the property of H function, we know that if only the equilibrium of system is not yet achieved, the H function is decrescent strictly. Let the function $L(f(t)) = H(f(t)) - H(f^{eq})$. It is obvious that we have

$$\Delta L(f(t + \delta t)) = L(f(t + \delta t)) - L(f(t)) \leq 0.$$

So, $-\Delta L$ is locally positive, semi-definite and L is a Lyapunov function. If the locally positive semi-definite condition is tenable, the system shows uniform local-asymptotic stability. In other words, L is uniformly stable and $L = 0$ is uniformly locally attractive. There exists δ at t such that $\|L(f(t))\| < \delta$ and $\lim_{t \rightarrow \infty} L(f(t)) = 0$. In a lattice Boltzmann system, if we can sustain the locally positive semi-definite of $-\Delta L$, we can enhance the stability of the lattice Boltzmann system. ELBM is just based on this theory to enhance the stability of lattice Boltzmann systems. As indicated in Section 1 there is non-existence of the H -theorem for the standard LBM (Yong and Luo, 2003, 2005). So, it is difficult to introduce the Lyapunov function into the standard LBM by H -theorem. From this view, ELBM is thermodynamically consistent and supported by the classical mathematical Lyapunov stability theory. So, ELBM is laudable and worth investigating further.

To establish the ELBM at the special lattice node, we need to discretise the entropic function at the special lattice velocity direction. The discretisation form of the entropy function Equation (2) by Gauss-Hermite quadrature formulas reads

$$\begin{aligned} S_d(f(x, t)) &= -\sum_{i=0}^n h_i(f_i(x, t)) \\ &= -\sum_{i=0}^n f_i(x, t) \ln(f_i(x, t) / w_i), \end{aligned} \quad (3)$$

where w_i is the weight associated with the i th particle of speed e_i and n is the total number of discrete velocity set at a grid node.

The macroscopic characteristics can be obtained via the distribution function solved from the following constraint optimisation problem

$$S_d(f) \rightarrow \max, \quad (4a)$$

and the corresponding constraint condition is

$$m(f) = M \quad (4b)$$

where M denotes the macroscopic characteristics of hydrodynamics such as density, moment and energy, and m is a function of microscopic state f_i . For the isothermal fluid flows, there are two macroscopic conservative variables

$$M = \{\rho, \vec{\rho}u\} = \{<1|f>, <\vec{e}|f>\}. \quad (5)$$

Introducing the corresponding Lagrange multipliers (μ, β) , the corresponding constraint optimisation problem of Equation (4) can be represented by the following problem (Ansumali and Karlin, 2001; Keating et al., 2007)

$$\delta \sum_{i=0}^n [h_i(f_i) - \mu f_i - \beta \cdot f_i e_i] = 0.$$

Calculating derivatives of the above extremum problem with respect to f_i yields

$$h_i'(f_i) = \mu + \beta \cdot e_i.$$

From the above extremum problem, we could obtain the following equilibrium distributions of ELBM for D2Q9 for 2D fluid flows (Karlin et al., 2007; Ansumali et al., 2003) (see Appendix for the details of velocity sets)

$$f_i^{eq} = \rho w_i \prod_{l=1}^2 (2 - \sqrt{1 + 3u_l^2}) \left(\frac{2u_l + \sqrt{1 + 3u_l^2}}{1 - u_l} \right)^{e_{il}/c}, \quad (6)$$

where c is the lattice speed and l is the index of the spatial directions. It is obvious that the equilibrium Equation (6) of ELBM is not a polynomial form and this form is different from the polynomial equilibrium of the standard LBM.

Now the lattice for the ELBM is concerned. For 3D fluid flow problems, ELBM needs a highly symmetric lattice (Ansumali et al., 2003; Chikatamarla et al., 2006). The discrete velocities involve all possible tensor products of three one-dimensional velocity sets (Ansumali et al., 2003; Chikatamarla et al., 2006). Thus for 3D case, the velocity number is up to 27 for D3Q27 (see Appendix for the details of velocity sets).

Another important characteristic of the ELBM is in the relaxation parameter. Unlike the standard LBM, the relaxation parameter γ in Equation (1) is adaptable to make the distributions of populations satisfy the monotonicity of H -theorem or entropy function. The monotonicity constraint on the entropy function is consisted of two steps (Tosi et al., 2006a): in the first step, populations are changed in the direction of the bare collision (Ansumali and Karlin, 2001), $\Delta_i = f_i^{eq} - f_i$, by such procedure the entropy function remains constant; in the second step, the dissipation is introduced and the magnitude of the entropy function increases. The effective relaxation frequency reads

$$\gamma = \alpha\beta, \quad (7)$$

where the parameter β is related to the relaxation time τ of the BGK model by the following formula (Ansumali et al., 2003; Karlin et al., 2003)

$$\beta = \delta t / (2\tau + \delta t). \quad (8)$$

The parameter α is obtained by solving the non-linear equation

$$S_d(f) = S_d(f + \alpha\Delta), \quad (9)$$

where α becomes a function of f . By solving Equation (9), we can get α . So, from Equations (7) and (8), we will obtain the modified relaxation frequency γ . Equation (9) guarantees uniform entropy and the monotonicity of the H -function. The corresponding effective viscosity ν is determined by

$$\nu_{\text{eff}}(\alpha) = c_s^2 \delta t \left(\frac{1}{\alpha\beta} - \frac{1}{2} \right), \quad (10)$$

where c_s is the lattice Mach number defined by

$$c^2 = 3RT = 3c_s^2. \quad (11)$$

It is obvious that the variance of α will lead to a change of the viscosity. Because of this basic property of ELBM, it is proved (Karlin et al., 2003) that the ELBM exhibits a sort of built-in subgrid models for turbulence flows. The scheme of ELBM reads

$$f_i(x + e_i \delta t, t + \delta t) - f_i(x, t) = \gamma(f_i^{\text{eq}}(x, t) - f_i(x, t)). \quad (12)$$

When we set $\alpha=2$, the above scheme is analogous to the standard LBM scheme. When $\beta \rightarrow 1$, the molecular viscosity will tend to vanish. So, the zero molecular viscosity limit corresponds to $\beta \rightarrow 1$. At the moment, the free degree of the system will increase very quickly and the eddy viscosity will dominate the flow field. The corresponding eddy viscosity will be adjusted by α . The eddy viscosity makes the extra dissipation act on the fluid flow system of the finite free degree and reduces the free degree of the fluid flow system. This action is the main property of ELBM and analogous to the action of the subgrid dissipation in Navier-Stokes systems. Let $\delta(\nu) = \nu_{\text{eff}}(\alpha) - \nu_{\text{eff}}(2)$. We will see that if $\delta(\nu) > 0$, this denotes that the effective viscosity is larger than that of the molecular viscosity. If $\delta(\nu) = 0$, the effective viscosity is identical with the molecular viscosity $\nu_{\text{eff}}(2)$. And if $\delta(\nu) < 0$, this case denotes that effective viscosity is smaller than the molecular viscosity. This case corresponds to a local micro-instability (Karlin et al., 2003).

The entropic scheme to determine the relaxation parameter can be summarised by the following two steps:

- Computation of the parameter β related to the viscosity $\nu_{\text{eff}}(2)$ by Equation (8).
- Computation of the parameter α by Equation (9).

The above procedure guarantees that for a given grid size, ELBM can be used to simulate the high Reynolds number fluid flows. The updating rule of the ELBM is the same as that of the standard LBM, and for the simplicity of presentation it is omitted here.

The ELBM has been proved to enhance stability due to its compliance with the H -theorem of kinetic theories, which guarantees the second law of the thermodynamics. However, the implementation of ELBM costs much time for solving the non-linear Equation (9). So, for the implementation of ELBM, enhancing the computational efficiency is an urgent problem.

3 Ehrenfests' coarse-graining idea

The Ehrenfests' idea for enhancing the stabilisation of the solution process of the lattice Boltzmann equation is to supplement the mechanical motion from the kinetic equation with periodic averaging in cells to produce piecewise constant, or coarse-grained, densities (Brownlee et al., 2006). In fact, this operation necessitates entropy production (Brownlee et al., 2006). The averaging in cells is an analogue of a kind of integration. The problem of the entropy maximum, Equation (9), is just a particular example because the entropy maximum makes the entropy to be locally constant.

From the Ehrenfests' idea (Brownlee et al., 2006), the entropy maximisation leads to an evolution equation for the macroscopic description. Here, we define Ehrenfests' chain as the sequence of quasi-equilibrium distribution functions $f^0, f^1, f^2, f^3, \dots$. Along the Ehrenfests' chain, the entropy increases. The entropy gain in a link in the chain is made up of two parts (Brownlee et al., 2006):

The entropy gain from mechanics motion.

The gain from the equilibration.

Owing to the successive entropy gain in the chain, the conversation systems become more and more dissipative (Brownlee et al., 2006). The increment in the macroscopic entropy is expressed by

$$\Delta S_d(f_i) = S_d(f_i^{\text{eq}}) - S_d(f_i). \quad (13)$$

It is obvious that zero increment is achieved when the system is in the equilibrium.

According to Ehrenfests' chain, we can approximate a solution of some coarse-grained macroscopic equations in a stepwise manner. The dissipation due to this chain is proportional to the relaxation time τ . By rearrangement

of Equation (12), the chain corresponding to the ELBM scheme reads

$$f_i(x + e_i \delta t, t + \delta t) = (1 - \beta) f_i(x, t) + \beta \tilde{f}_i(x, t), \quad (14)$$

where $\tilde{f}_i(x, t) = (1 - \alpha) f_i(x, t) + \alpha f_i^{eq}(x, t)$ and α is a function of f_i . α could be adjusted to make a constant entropy condition being satisfied (Brownlee et al., 2006). Now, we show Ehrenfests' updating step according to an entropic threshold as follows,

$$f_i(x + e_i \delta t, t + \delta t) = \begin{cases} (1 - \gamma) f_i(x, t) + \gamma f_i^{eq}(x, t), & \Delta S_d(f_i) > \sigma \\ (1 - \gamma) f_i(x, t) + \gamma \tilde{f}_i(x, t), & \Delta S_d(f_i) \leq \sigma \end{cases}, \quad (15)$$

where σ is the entropic threshold. The scheme of Equation (15) does not need to solve Equation (9) at every lattice node, but can guarantee the entropic increase (Brownlee et al., 2006).

4 Positivity-enforcing LBM scheme

To improve the stability of LBM, by avoiding any negativeness of the distribution function f_i , a scheme, called positivity-enforcing LBM, is described by Li et al. (2004).

$$\tau' = \max_{i=0, \dots, n}(\tau, 1 - f_i^{eq}/f_i), \quad (16)$$

where $\gamma = 1/\tau'$. The truncated error of the equilibrium distribution f_i^{eq} in Equation (16) is up to fourth order (Chen and Teixeira, 2000). Normally, for the standard LBM, the truncated error is up to third order. The expression of f_i^{eq} in the positivity-enforcing LBM scheme is as follows

$$f_i^{eq} = \rho w_i \left\{ 1 + \frac{e_i \cdot u}{c_s^2} + \frac{1}{2} \frac{(e_i \cdot u)^2}{c_s^4} - \frac{1}{2} \frac{u^2}{c_s^4} + \frac{1}{6} \frac{(e_i \cdot u)^3}{c_s^6} - \frac{1}{2} \frac{(e_i \cdot u)}{c_s^4} u^2 \right\}.$$

In this way, positive post-collision state distributions are preserved as long as pre-collision distributions are positive. In the section of numerical tests, the positivity-enforcing LBM will be implemented based on the above distribution and some comparison will be made with the optimised ELBM scheme.

5 Entropic function

To check the results of numerical simulations, the time evolution of the global entropy should be checked. In each time step, the following quantity is calculated

$$S(t) = - \sum_x \sum_{i=0}^b f_i(x, t) \ln(f_i(x, t) / w_i). \quad (17)$$

By some simple algebra, we obtain

$$\begin{aligned} S(t) &= - \sum_x \sum_{i=0}^b f_i(x, t) \ln(f_i(x, t) / f_i^{eq}(x, t)) \\ &\quad - \sum_x \sum_{i=0}^b f_i(x, t) \ln(f_i^{eq}(x, t) / w_i) \\ &= - \sum_x \sum_{i=0}^b f_i(x, t) \ln(f_i(x, t) / f_i^{eq}(x, t)) \\ &\quad - \sum_x \sum_{i=0}^b f_i^{eq}(x, t) \ln(f_i^{eq}(x, t) / w_i) \\ &\quad + \sum_x \sum_{i=0}^b (f_i^{eq}(x, t) - f_i(x, t)) \ln(f_i^{eq}(x, t) / w_i). \end{aligned} \quad (18)$$

For convenience, we introduce the following formulations

$$S(f, f') = - \sum_x \sum_{i=0}^b f_i \ln(f_i / f'_i), \quad (19)$$

$$S_k(f, f') = - \sum_x \sum_{i=0}^b (f_i - f'_i) \ln(f_i / w_i). \quad (20)$$

Then, we have the following compact expression

$$S(t) = S(f, f^{eq}) + S(f^{eq}, w) + S_k(f^{eq}, f). \quad (21)$$

$S(f, g)$ is the Kullback entropy (relative entropy) belonging to the family of Massieu-Planck-Kramers functions, which measures the distance between two 'rays', f and g (Brownlee et al., 2008). Here, the Kullback entropy is expressed in quadratic approximation (Brownlee et al., 2008)

$$\begin{aligned} S(f, f^{eq}) &= - \sum_x \sum_{i=0}^n f_i \ln(f_i / f_i^{eq}) \\ &\approx - \sum_x \sum_{i=0}^n \frac{(f_i - f_i^{eq})^2}{f_i^{eq}}. \end{aligned} \quad (22)$$

In the section of numerical tests, we will check the entropy for optimisation strategies.

6 Optimisation strategy

For enhancing efficiency of ELBM, Tosi et al. (2006b) proposed a good idea to save the computational cost. But in their paper, the optimisation strategies focus on special problems. In this paper, we adopt the entropy threshold to optimise the implementation of ELBM. The strategy for solving Equation (9) is as follows.

The initial value for solving Equation (9) is adopted as follows (Tosi et al. 2006a):

$$\alpha^t = \begin{cases} \alpha^{t-\delta t}, & t > 0 \\ 2, & t = 0 \end{cases}. \quad (23)$$

Newton-Raphson bisection computational method is adopted to solve Equation (9). The threshold of entropy σ

is chosen to determine whether Equation (9) should be solved. When $\Delta S_d \leq \sigma$, we solve the Equation (9); otherwise, we set $\alpha' = 2$.

7 Numerical tests

In this section, we will carry out some numerical tests to validate the optimisation strategy of ELBM. The numerical tests include: a 2D lid-driven cavity fluid flow; a 2D backward-facing step fluid flow; a 3D backward-facing step fluid flow. The lattice schemes are D2Q9 and D3Q27 for 2D and 3D fluid flow problems, respectively. The L^q ($q = 1, 2$) convergence tolerances for 2D problems are defined by Hou et al. (1995).

$$E_1^i = \frac{\sum_x [|u^i - u^{i-1}| + |v^i - v^{i-1}|]}{\sum_x |u^{i-1} + v^{i-1}|} \leq \varepsilon_1 \tag{24}$$

and

$$E_2^i = \frac{\sqrt{\sum_x [|u^i - u^{i-1}|^2 + |v^i - v^{i-1}|^2]}}{\sqrt{\sum_x |u^{i-1} + v^{i-1}|^2}} \leq \varepsilon_2, \tag{25}$$

where ε_1 and ε_2 are very small real numbers.

7.1 2D lid-driven cavity fluid flow

This is a steady, incompressible fluid flow within a square cavity caused by a moving lid for not very high Reynolds numbers (Re). Numerical simulations are conducted for Re = 2000, 3200. The top boundary moves from left to right with a constant velocity $U = (0.1, 0)$. The initial density $\rho = 1.0$. The lattice size is 100 by 100. In the numerical simulations, the Maxwell diffusive boundary condition is considered (Ansumali and Karlin, 2002).

The simulation results of the stream functions with the optimisation strategy of ELBM are shown in Figure 1 and Figure 2 for Re = 2000 and Re = 3200, respectively. In Figure 3, our predicted u and v velocity distributions for Re = 3200 are compared with the results of benchmarks (Ghia et al., 1982). From the results, we can see that the details of vortex structures are revealed and the agreement in velocity distributions is quite satisfactory.

Figure 1 Streamline for Re = 2000

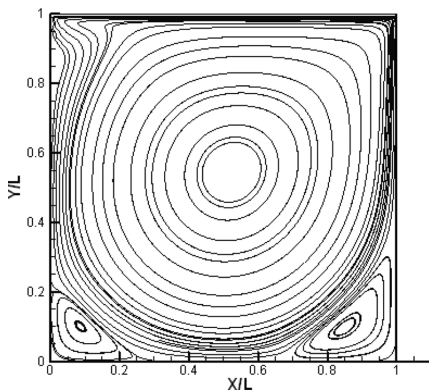


Figure 2 Streamline for Re = 3200

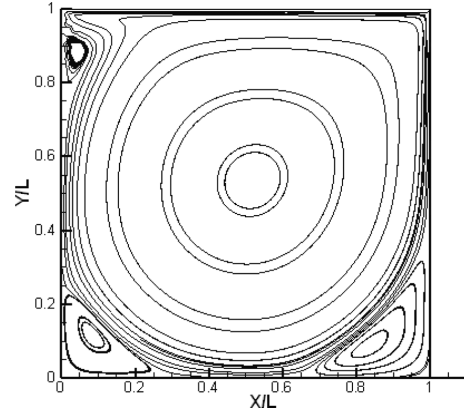
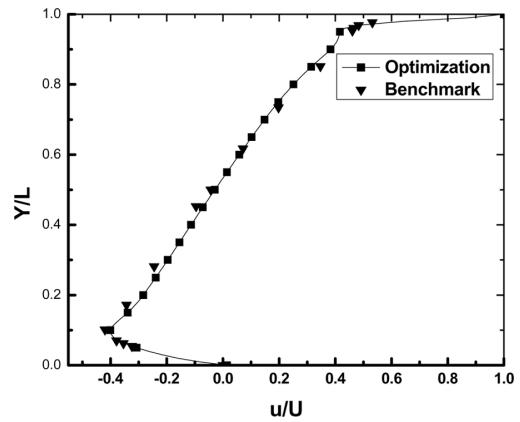
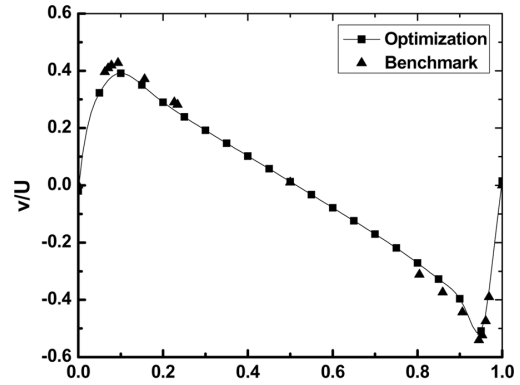


Figure 3 Re = 3200, the results of benchmark and optimisation:

- (a) u -velocity profile along the vertical centreline,
- (b) v -velocity profile along the horizontal centreline



(a)



(b)

The values of ε_1 and ε_2 in Equations (24) and (25) are listed in Table 1. They are achieved in 5000th step and 7000th step for Re = 2000 and Re = 3200, respectively. In Figures 4 and 5, the evolution of the global entropy and global Kullback entropy are presented. From the figures, we can see that the global entropy gradually increases and achieves its maximum value, and the global Kullback entropy gradually decreases and achieves its minimum value. The stable solutions are achieved when two kinds of entropy gain the corresponding extremum.

Figure 4 Global entropy evolution

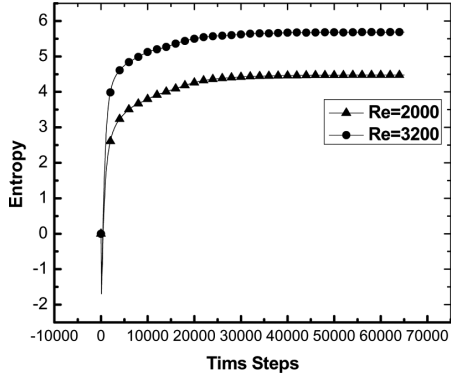


Figure 5 Global Kullback entropy evolution

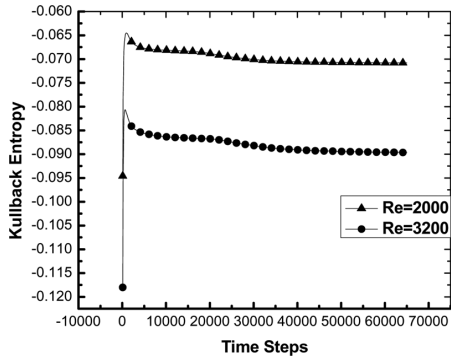


Table 1 Convergence errors

Re	E_1^i	E_2^i
2000	5.349E-6	5.741E-6
3200	6.502E-6	6.450E-6

Now, attention is turned to the cost of computational time. The optimisation strategy makes the procedure of computations shortened. The optimised ELBM costs 2999s compared with 2713s for the positivity-enforcing method ($Re = 2000$) and 2934s compared with 2683s for the positivity-enforcing method ($Re = 3200$). The CPU time cost of the optimised ELBM is almost the same as the positivity-enforcing method under the same convergence tolerances. On the other hand, the optimised ELBM has much higher convergence rate than ELBM. Also, since ELBM allows to increase the Reynolds number by nearly an order of magnitude, given that CPU time scales like Re^4 (in 3D), it appears that the direct simulation of high Reynolds flows is most conveniently handled by the optimised ELBM rather than the positivity-enforcing method (Tosi et al., 2006b).

It is proved that ELBM is a built-in subgrid method (Karlin et al., 2003). To verify this interpretation, we implement the computation of a 2D lid-driven flow with a very high Reynolds number up to 5000 and 7500. The lattice sizes are 128 by 128 and 160 by 160, respectively. The top velocity $U = (0.01, 0)$. For the standard LBM, this simulation is very difficult to be implemented. The stream function of the two cases are

provided in Figures 6 and 7, and in Figure 8 the velocity distributions are shown. It can be seen that the ELBM can simulate the lid-driven fluid flows of the high Reynolds numbers on very coarse meshes. On the contrary, the standard LBM could hardly implement the simulations on such coarse meshes. For high Reynolds number fluid flows, the phenomenon of fluid flows is very complicated (Bruneau and Saad, 2006; Garcia, 2007). So, there exist some differences between the solutions of ELBM and Ghia et al. (1982). From this view of the built-in subgrid method, ELBM is a more effective method than the standard LBM for high Reynolds number fluid flows.

Figure 6 Streamline for $Re = 5000$ (lattice: 128 by 128)

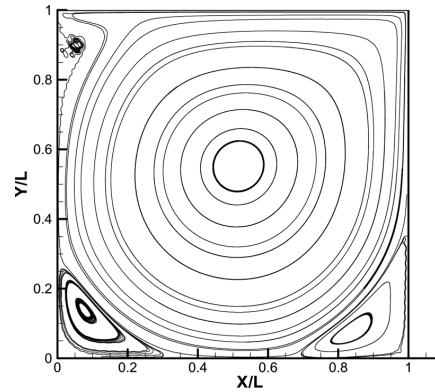


Figure 7 Streamline for $Re = 7500$ (lattice: 160 by 160)

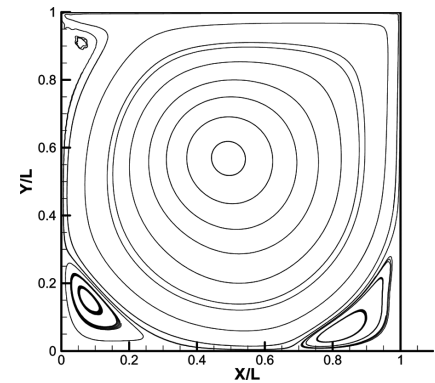
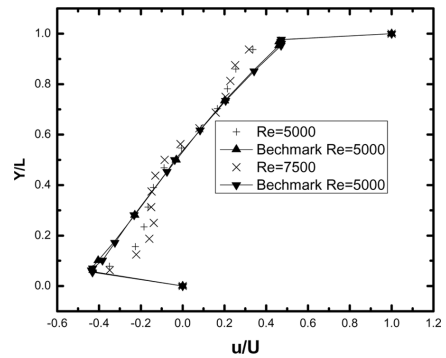
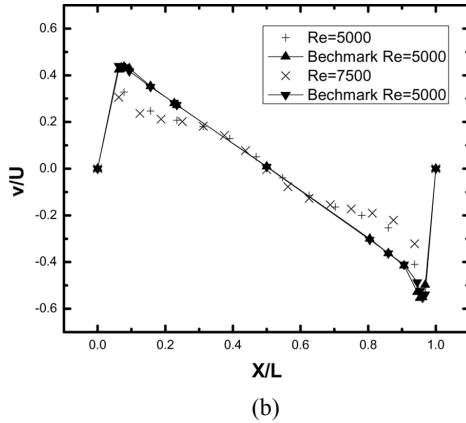


Figure 8 $Re = 5000$ and $Re = 7500$, the results of benchmark and optimisation: (a) u -velocity profile along the vertical centreline and (b) v -velocity profile along the horizontal centreline (continues on next page)



(a)

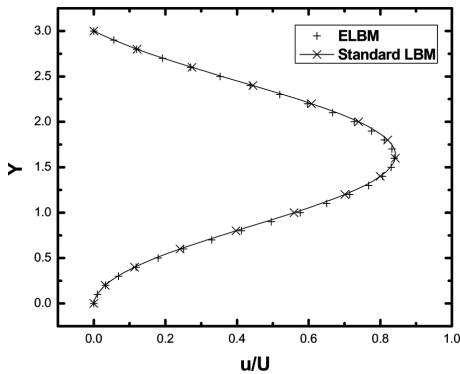
Figure 8 Re = 5000 and Re = 7500, the results of benchmark and optimisation: (a) u-velocity profile along the vertical centreline and (b) v-velocity profile along the horizontal centreline (continued)



7.2 2D Backward-facing step fluid flow

In this section, we implement ELBM for an open system of a 2D backward-facing step fluid flow based on the optimisation strategy in Section 6. By this example, we just want to show that the ELBM with the optimisation strategy is valid for open systems. The channel length and channel width is 20 and 3, respectively. The step width and height is 5 and 1. The inlet velocity profile is parabolic. The average velocity $u_{mean} = 0.15$. The definition of backward-facing step fluid flow Reynolds number is $Re = 2u_{mean}h/\nu$ (h denotes the step height). In this simulation, $Re = 200$ and the channel expansion ratio $ER = 1.5$. The resolutions of ELBM and LBM are 0.1 and 0.05, respectively. By the computational prediction, the reattachment lengths are 6.1056 and 6.4014. Meanwhile, from Figures 9 and 10, we see that the ELBM with the optimisation strategy can simulate the backward-facing step fluid flow very well.

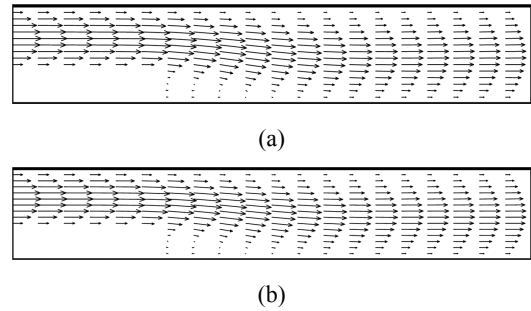
Figure 9 u-velocity profile along the vertical line at Y = 10



It is very clear that from 2D fluid flows the ELBM with the optimisation strategy can simulate the fluid flow problems very well. Moreover, ELBM does not need very fine meshes compared with the standard LBM. All of these are attributed to the built-in subgrid property of ELBM. For the standard LBM, the relaxation frequency is kept

invariant. So, the corresponding viscosity in the standard LBM is invariant and describes the molecular viscosity. We know that for high Reynolds number fluid flows, if the spatial grid-free degree is not enough to catch the small-scale information, we need to modify the viscosity of the fluid flow model to enhance the dissipation of fluid flow systems and smear out the small-scale information. The subgrid model established in macroscopic Navier-Stokes equations enhances dissipation by adding an eddy viscosity term. Generally, this eddy viscosity term modifies the molecular viscosity and makes the effective viscosity to be changed according to the characteristics of flow fields. Normally, this term added into macroscopic Navier-Stokes equations is experimental, especially, for the related parameters. But, ELBM enhances the dissipation of high Reynolds number flows by H function. From this view, ELBM has the profoundly physical consistency and can adjust viscosity to enhance dissipation by the second law of thermodynamics. And there does not exist any experimental parameter. So, ELBM plays a physically consistent subgrid role for high Reynolds number fluid flows.

Figure 10 Velocity vectors: (a) velocity vector by ELBM and (b) velocity vector by the standard LBM



7.3 3D backward-facing step channel fluid flow

In this section, we implement the ELBM with the optimisation strategy for a 3D fluid flow problem. A typical example we chose is a 3D transitional backward-facing step channel fluid flow. The fluid flow domain is constructed in a cuboid $[0, 20] \times [0, 3] \times [0, 4]$. The Reynolds number is defined by $Re = 2u_{mean}h/\nu = 1000$. The step width is equal to 5.0 and the step height is equal to 1. The spatial resolution scale is 0.05. The time step interval is equal to 0.0075. Except inlet and outlet boundaries, other boundaries possess a non-slip boundary condition. The computational results are shown in Figures 11–14. The number of computational step is up to 2666 time steps. The corresponding time $t = 19.995$. According to the results of ELBM simulation, it is clear that although the geometry of the backward-facing step is simple, there exist complex physical phenomena. The physical complexity is attributed to the presence of eddies near the step wall (Rani et al., 2007). ELBM can simulate these 3D complex physical phenomena very well. All of these demonstrate the validity of ELBM with the optimisation strategy.

Figure 11 Iso-surfaces of u , v and w : (a) $u = -0.0237$; (b) $v = 0.0138$ and (c) $w = 0.0148$

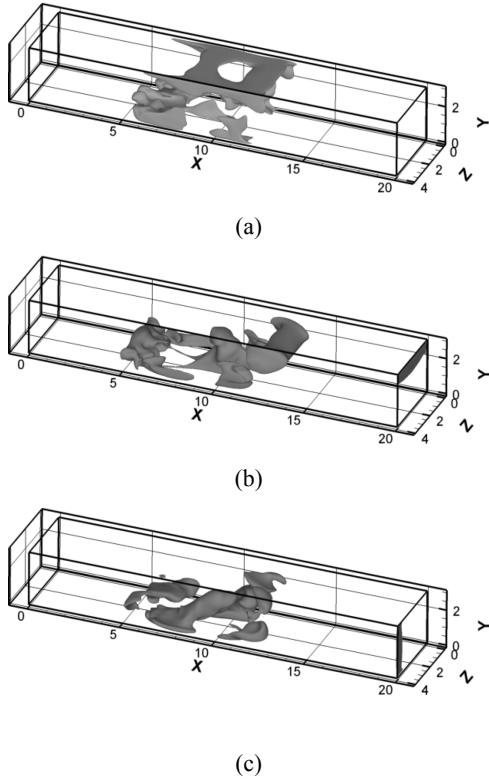


Figure 12 Velocity norm magnitude slice at $z = 2$

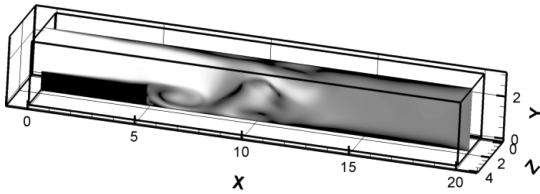


Figure 13 Iso-surfaces of vorticity vectors: (a) magnitude of x component of vorticity = 0.0065; (b) magnitude of y component of vorticity = 0.013 and (c) magnitude of z component of vorticity = 0.0054 (continues on next column)

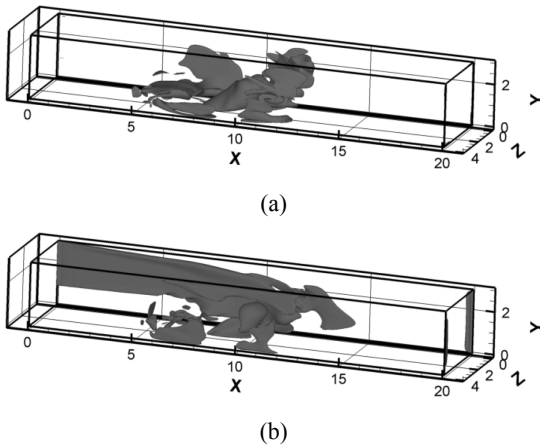


Figure 13 Iso-surfaces of vorticity vectors: (a) magnitude of x component of vorticity = 0.0065; (b) magnitude of y component of vorticity = 0.013 and (c) magnitude of z component of vorticity = 0.0054 (continued)

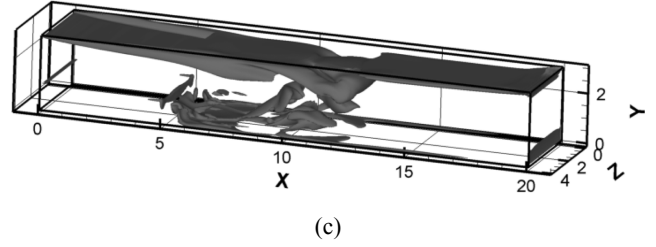
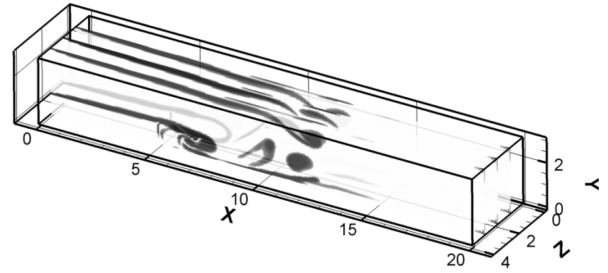


Figure 14 Vorticity norm magnitude slices at $z = 1, 2,$ and 3



8 Conclusion

In this paper, we investigate the two kinds of fluid flow problems by ELBM. It is known that there exists an infamous limitation about the standard LBM for low viscosities. ELBM with the optimisation strategy alleviates this limitation and saves the computational cost. ELBM needs to solve a non-linear equation at every lattice site and costs much time to implement the numerical simulations. Although some optimisation methods are proposed, there still exist some restrictions to enlarge the applications. We turn to Ehrenfest's coarse-graining idea and restrict the solving of the non-linear equation to some special points at which the local entropy decreases (below some threshold values). By this method, we could save the computational time and also get the correct numerical approximate solutions. By numerical illustrations, we verify ELBM with the optimisation strategy for 2D and 3D fluid flow problems. These tests demonstrate the validity of ELBM as a tool for high Reynolds number simulations. In all, ELBM is an effective and high-stable method for the high Reynolds fluid flows.

Acknowledgement

Supported by National Natural Science Key Fund (Grant No. 50636050). Illuminating discussions and helps with Francesca Tosi are acknowledged by the first author. The partial simulations were performed in National High Performance Computing Center in Xi'an Jiaotong University.

References

- Ansumali, S. and Karlin, I.V. (2000) 'Stabilization of the lattice Boltzmann method by the H theorem: A numerical test', *Phys. Rev. E*, Vol. 62, pp.79–99.
- Ansumali, S. and Karlin, I.V. (2001) 'Entropy function approach to the lattice Boltzmann method', *J. Stat. Phys.*, Vol. 107, pp.291–308.
- Ansumali, S. and Karlin, I.V. (2002) 'Kinetic boundary conditions in the lattice Boltzmann method', *Phys. Rev. E*, Vol. 66, pp.026311-1-6.
- Ansumali, S., Karlin, I.V. and Ottinger, H.C. (2003) 'Minimal entropic kinetic models for hydrodynamics', *Europhys. Lett.*, Vol. 63, No. 6, pp.798–804.
- Boghosian, B.M., Yezpez, J., Coveney, V.P. and Wagner, A.J. (2001) 'Entropy lattice Boltzmann methods', *Proc. R. Soc. London. Ser. A*, Vol. 457, pp.717–766.
- Brownlee, R.A., Gorban, A.N. and Levesley, J. (2006) 'Stabilization of the lattice Boltzmann method using the Ehrenfests' coarse-graining idea', *Phys. Rev. E*, Vol. 74, pp.037703-1-4.
- Brownlee, R.A., Gorban, A.N., Levesley, J. (2008) 'Nonequilibrium entropy limiters in lattice Boltzmann methods', *Physica A: Statistical Mechanics and Its Applications*, Vol. 387, Nos. 2–3, pp.385–406.
- Bruneau, C.H. and Saad, M. (2006) 'The 2D lid-driven cavity problem revisited', *Comput. Fluids*, Vol. 35, pp.326–348.
- Chapman, S. and Cowling, T.G. (1970) *The Mathematical Theory of Non-uniform Gases*, 3rd ed., Cambridge University Press, Cambridge, UK, pp.67–85.
- Chen, S. and Doolen, G. (1998) 'Lattice Boltzmann method for fluid flow', *Annu. Rev. Fluid Mech.*, Vol. 30, pp.329–364.
- Chen, H., Kandasamy, S., Orszag, S., Shock, R., Succi, S. and Yakhot, V. (2003) 'Extended Boltzmann kinetic equation for turbulent flows', *Science*, Vol. 301, pp.633–636.
- Chen, H. and Teixeira, C. (2000) 'H-theorem and origins of instability in thermal lattice Boltzmann models', *Comput. Phys. Commun.*, Vol. 129, pp.21–31.
- Chikatamarla, S.S., Ansumali, S. and Karlin, I.V. (2006) 'Entropy lattice Boltzmann models for hydrodynamics in three dimensions', *Phys. Rev. Lett.*, Vol. 97, pp.010201-1-4.
- Garcia, S. (2007) 'The lid-driven square cavity flow: from stationary to time periodic and chaotic', *Commun. Comput. Phys.*, Vol. 2, No. 5, pp.900–932.
- Ghia, U., Ghia, K.N. and Shin, C.T. (1982) 'High-resolutions for incompressible flow using the Navier-Stokes equations and a multigrid method', *J. Comput. Phys.*, Vol. 48, pp.387–411.
- He, X. and Li, N. (2000) 'Lattice Boltzmann simulation of electro-chemical systems', *Comput. Phys. Commun.*, Vol. 129, pp.158–166.
- Hou, S., Zou, Q., Chen, S., Doolen, G. and Cogley, A.C. (1995) 'Simulation of cavity flow by the lattice Boltzmann method', *J. Comput. Phys.*, Vol. 11, pp.329–347.
- Karlin, I.V., Ansumali, S., Deangelis, E., Ottinger, H.C. and Succi, S. (2003) *Entropic Lattice Boltzmann Method for Large Scale Turbulence Simulation*, e-print: <http://arXiv.org/abs/condmat/0306003>
- Karlin, I.V., Chikatamarla, S.S. and Ansumali, S. (2007) 'Elements of the lattice Boltzmann method II: kinetic and hydrodynamics in one dimension', *Commun. Comput. Phys.*, Vol. 2, No. 2, pp.196–238.
- Keating, B., Vahala, G., Yezpez, J., Soe, M. and Vahala, L. (2007) 'Entropy lattice Boltzmann representations required to recover Navier-Stokes flows', *Phys. Rev. E*, Vol. 75, pp.036712-1-11.
- Li, Y., Shock, R., Zhang, R. and Chen, H. (2004) 'Numerical study of flow past an impulsively started cylinder by the lattice Boltzmann method', *J. Fluid Mech.*, Vol. 519, pp.273–300.
- Qian, Y.H., d'Humieres, D. and Lallemand, P. (1992) 'Lattice BGK models for Navier-Stokes equation', *Europhys. Lett.*, Vol. 17, No. 6, pp.479–485.
- Rani, H.P., Sheu, T.W.H. and Tsai, E.S.F. (2007) 'Eddy structures in a transitional backward-facing step flow', *J. Fluid Mech.*, Vol. 588, pp.43–58.
- Rothman, D.H. and Zaleski, S. (1994) 'Lattice gas models of phase separation: interface, phase transition, and multiphase flow', *Rev. Mod. Phys.*, Vol. 66, No. 4, pp.1417–1479.
- Shan, X. and He, X. (1998) 'Discretization of the velocity space in the solution of the Boltzmann equation', *Phys. Rev. Lett.*, Vol. 80, pp.65–68.
- Succi, S. (2001) *The Lattice Boltzmann Equation for Fluid Dynamics and Beyond*, Oxford University Press, USA, New York.
- Takada, N., Misawa, M., Tomiyama, A. and Hosokawa, S. (2001) 'Simulation of bubble motion under gravity by lattice Boltzmann method', *J. Nuc. Sci. Tech.*, Vol. 38, No. 5, pp.330–341.
- Temam, R. (2000) *Infinite-dimensional Dynamical Systems in Mechanics and Physics*, Springer-Verlag, New York, Berlin, Heidelberg, pp.335–379.
- Tosi, F., Ubertini, S., Succi, S. and Karlin, I.V. (2006a) 'Optimization strategies for the lattice entropy lattice Boltzmann method', *J. Sci. Comput.*, Vol. 30, No. 3, pp.369–387.
- Tosi, F., Ubertini, S., Succi, S., Chen, H. and Karlin, I.V. (2006b) 'Numerical stability of entropy versus positivity-enforcing lattice Boltzmann schemes', *Math. Comput. Simulat.*, Vol. 72, pp.227–231.
- Yong, W.A. and Luo, L.S. (2003) 'Nonexistence of H-theorems for the athermal lattice Boltzmann models with polynomial equilibria', *Phys. Rev. E*, Vol. 67, pp.051105-1-4.
- Yong, W.A. and Luo, L.S. (2005) 'Nonexistence of H theorem for some lattice Boltzmann models', *J. Stat. Phys.*, Vol. 121, pp.91–103.

Appendix

A: D2Q9 model

Lattice nodes:

$$X = \{0, -1, -1, -1, 0, 1, 1, 1, 0\}$$

$$Y = \{0, 1, 0, -1, -1, -1, 0, 1, 1\}$$

Weight:

$$W = \{4/9, 1/36, 1/9, 1/36, 1/9, 1/36, 1/9, 1/36, 1/9\}$$

B: D3Q27 model

Lattice nodes:

$$X = \{0, -1, 0, 0, -1, -1, -1, -1, 0, 0, -1, -1, -1, -1, 1, 0, 0, 1, 1, 1, 1, 0, 0, 1, 1, 1, 1\}$$

$$Y = \{0, 0, -1, 0, -1, 1, 0, 0, -1, -1, -1, -1, 1, 1, 0, 1, 0, 1, -1, 0, 0, 1, 1, 1, 1, -1, -1\}$$

$$Z = \{0, 0, 0, -1, 0, 0, -1, 1, -1, 1, -1, 1, -1, 1, 0, 0, 1, 0, 0, 1, -1, 1, -1, 1, -1, 1, -1\}$$

Weight:

$$W = \{8/27, 2/27, 2/27, 2/27, 1/54, 1/54, 1/54, 1/54, 1/54, 1/54, 1/216, 1/216, 1/216, 1/216, 2/27, 2/27, 2/27, 1/54, 1/54, 1/54, 1/54, 1/54, 1/216, 1/216, 1/216, 1/216\}$$